Journal of the Korean Ceramic Society
Vol. 54, No. 5, pp. 422~428, 2017.

https://doi.org/10.4191/kcers.2017.54.5.09

Structural and Optical Properties of Yellow-Emitting $CaGd_2ZrSc(AlO_4)_3:Ce^{3+}$ Phosphor for Solid-State Lighting

Yoon Hwa Kim, Bo Young Kim, Noolu S. M. Viswanath, Paulraj Arunkumar, and Won Bin Im†

School of Materials Science and Engineering and Optolelectronics Convergence Research Center, Chonnam National University, Gwangju 61186, Korea

(Received July 3, 2017; Revised August 13, September 8, 2017; Accepted September 8, 2017)

ABSTRACT

Single-phase yellow phosphor, $CaGd_{2-x}ZrSc(AlO_4)_3:xCe^{3+}$ (CGZSA:Ce^{3+}), possessing cubic symmetry with varied Ce^{3+} concentrations, was synthesized using the solid-state reaction method. The samples were characterized using X-ray diffraction (XRD), excitation spectra, emission spectra, thermal quenching, and decay curves. The cubic phase of CGZSA:Ce^{3+} phosphor was confirmed *via* XRD analysis. The photoluminescence spectra of CGZSA:Ce^{3+} phosphor demonstrated that the phosphor could be excited at the wavelength of 440 nm; a broad yellow emission band was centered at 541 nm. These results indicate that the phosphors are adequately excited by blue light and have the potential to function as yellow-emitting phosphors for applications in white light-emitting diodes.

Key words : Garnet structure, Yellow-emitting phosphor, White LEDs

1. Introduction

Phosphor-converted white light-emitting devices (pc-WLEDs) are considered a promising light source for solid-state lighting, displays, and headlights owing to their high efficiency, low energy consumption, long life, and environmentally benign nature.[1] Commercial pc-WLEDs are fabricated by incorporating $Y_3Al_5O_{12}:Ce^{3+}$ phosphor (YAG:Ce^{3+}) as an emissive layer under blue LED excitation; this process was initiated by Nichia Corporation.[2,3] The dominance of pc-WLEDs in lighting applications is due to the invention of efficient blue LEDs.[4] The broadband activators (Eu^{2+} and Ce^{3+}), especially Ce^{3+}, are the most promising activators for phosphors owing to their broad emission band originating from the 4*f*-5*d* transitions.[5,6] They can extend the absorption band from ultraviolet (UV) to the visible region in the phosphor hosts, matching the most efficient excitation source, the InGaN blue-LED chip.[6]

Garnet-based phosphors are the most commonly utilized phosphor hosts (such as YAG:Ce^{3+}) with the formula unit $X_3Y_2(ZO_4)_3$ belonging to the *Ia*-3*d* space group,[7] wherein the three crystallographic cation sites, namely *X*, *Y*, and *Z*, form eight-, six-, and four-coordinations to form a dodecahedron, octahedron, and tetrahedron, respectively.[8] Moreover, Ce^{3+}-based garnet phosphors have shown interesting optical properties such as broad emission in the visible region, ranging from green ($Ca_3Sc_2(SiO_4)_3:Ce^{3+}$) to yellow (YAG:$Ce^{3+}$) to orange-red ($Lu_2CaMg_2(Si,Ge)_3O_{12}:Ce^{3+}$).[9-11] The large crystal field splitting of the ^2D level of Ce^{3+} ion in the garnet structure produces emission and excitation at relatively longer wavelengths, especially in the visible region, rendering it an exceptional phosphor host for WLED lighting.[10]

A novel aluminate garnet $Ca_2GdZr_2(AlO_4)_3:Ce^{3+}$ phosphor was recently reported with broad absorption ranging from the UV to blue regions and broad cyan emission peaking at 510 nm. Tuning of the emission properties of $Ca_2MZr_2(AlO_4)_3:Ce^{3+}$ (M = Lu^{3+}, Y^{3+}, Gd^{3+}) phosphor from blue (480 nm) to cyan (500 nm) with the increase in the ionic radii of M^{3+} ion was reported.[12] The splitting of the cubic crystal field ^2E_g energy level in $Ca_2MZr_2(AlO_4)_3:Ce^{3+}$ increased with the increase in the ionic radii of M^{3+}, which dominated the spectroscopic red-shift emission.[12] Based on the $Ca_2GdZr_2(AlO_4)_3:Ce^{3+}$ phosphor, with a maximum emission wavelength of 500 nm, Zr^{4+} of the *Y* site was replaced with Sc^{3+}, and Ca^{2+} of the *X* site was replaced with Gd^{3+} to obtain the $CaGd_2ZrSc(AlO_4)_3:Ce^{3+}$ (CGZSA:Ce^{3+}) phosphor with a maximum emission wavelength of 545 nm. The yellow emission in the CGZSA:Ce^{3+} phosphor originates from the increase in the splitting of the ^2E_g energy level owing to the decrease in the covalent character of Ce-O.[12] A new yellow-emitting $CaGd_2ZrSc(AlO_4)_3:Ce^{3+}$ (CGZSA:Ce^{3+}) garnet phosphor under blue excitation has been reported. However, the effect of Ce^{3+} concentration on the structural and optical properties of the CGZSA:Ce^{3+} phosphor has not been reported yet.

In this study, Ce^{3+}-doped aluminate garnet phosphors containing zirconium were synthesized using the solid-state reaction method. To understand the detailed ionic distribution in these garnet crystals, the structure of the representative compound CGZSA:Ce^{3+} was determined. The photoluminescence (PL) properties of these CGZSA:Ce^{3+} phos-

†Corresponding author : Won Bin Im
E-mail : imwonbin@jnu.ac.kr
Tel : +82-62-530-1715 Fax : +82-62-530-1699

phors were presented and analyzed based on the crystal structure. The thermal stability and quantum efficiency were investigated in detail.

2. Experimental Procedure

Different Ce^{3+} concentrations of $CaGd_{2-x}ZrSc(AlO_4)_3:xCe^{3+}$ (abbreviated as CGZSA:xCe^{3+}) yellow-emitting phosphors were synthesized using the solid-state reaction method with $CaCO_3$ (Aldrich, 99.99%), Gd_2O_3 (Aldrich, 99.9%), ZrO_2 (Aldrich, 99.99%), Sc_2O_3 (Kojundo, 99.9%), α-Al_2O_3 (Kojundo, 99.99%), and CeO_2 (Kojundo, 99.99%) as the precursors. The precursors in stoichiometric ratios were mixed using an agate mortar for 30 min, with acetone as the dispersing medium, to obtain homogeneous mixtures. The mixtures were placed in an alumina crucible and sintered at 1450°C for 4 h at a heating rate of 5°C/min under a reducing atmosphere (N_2/H_2 = 95% : 5%) in a tube furnace. Subsequently, the samples were gradually cooled to room temperature in the furnace and, finally, these samples were ground into powders to obtain a series of samples of CGZSA:xCe^{3+} with different Ce^{3+} concentrations (x = 0.01, 0.02, 0.04, 0.05, 0.06, and 0.07).

The composition and phase purity of the samples were identified using X-ray diffraction (XRD). XRD patterns were obtained using CuKα radiation (Philips X'Pert) over the angle range of $10° \le 2\theta \le 100°$. Diffraction data were analyzed *via* Rietveld refinement using the general structure analysis system (GSAS) software.[13] Room-temperature PL excitation and emission spectra were obtained using a Hitachi F-4500 fluorescence spectrophotometer in the wavelength range of 300 - 700 nm. The thermal quenching (TQ) characteristics were measured in the temperature range of 25 - 200°C by connecting the Hitachi F-4500 fluorescence spectrometer to an integrated heater, temperature controller, and thermal sensor. At the temperature of −196°C, low-temperature PL spectra were obtained using a Hitachi F-7000 luminescence spectrophotometer under excitation at 325 nm connected to the ARS-cryostat system at the Korea Photonic Technology Institute (KOPTI), Republic of Korea. The fluorescence decay curve was obtained using a Horiba Fluorolog-3 with a 450 nm LED. The quantum yield (QY) of the phosphors was measured using a QY measurement system (Hamamatsu C9920-02) at the KOPTI, Republic of Korea.

3. Results and Discussion

Figure 1(a) shows the results of the Rietveld refinement of the XRD data profiles of CGZSA:0.04Ce^{3+}. The crystal structure of $Ca_2GdZr_2(AlO_4)_3$[12] (CGZSA) was considered as the starting model for the Rietveld refinements. The residual factor was R_{wp} = 2.60% and the goodness-of-fit parameter (χ^2) was 2.261. When Ce^{3+} was doped into the CGZSA host lattice, the obtained sample consisted of a single phase with no impurity phases present. The diffraction pattern revealed a general cubic garnet-type structure belonging to the space group of Ia-3d (#230) with cations in special positions (24c, 16a, and 24d sites) and oxygen anions in general positions (96h site). Crystallographic parameters from the Rietveld refinement provided the cell parameters of $a = b = c$ = 12.46417(5) Å. The structural parameters, such as the interatomic distance and the bond valence sums (BVS)[14] are listed in Tables 1, 2, and 3. The structure has many shared edges between adjacent polyhedrals. In the CGZSA:0.04Ce^{3+} structure, the AlO_4 tetrahedron and the $(Zr/Sc)O_6$ octahedron share their edges with two and six triangular $(Ca/Gd/Ce)O_8$ dodecahedra, respectively [Fig. 1(b)]. The triangular dodecahedron shares its edges with two tetrahedra, four octahedra, and four other triangular dodecahedra. Tetrahedra and octahedra are linked through the sharing of all corners.[15]

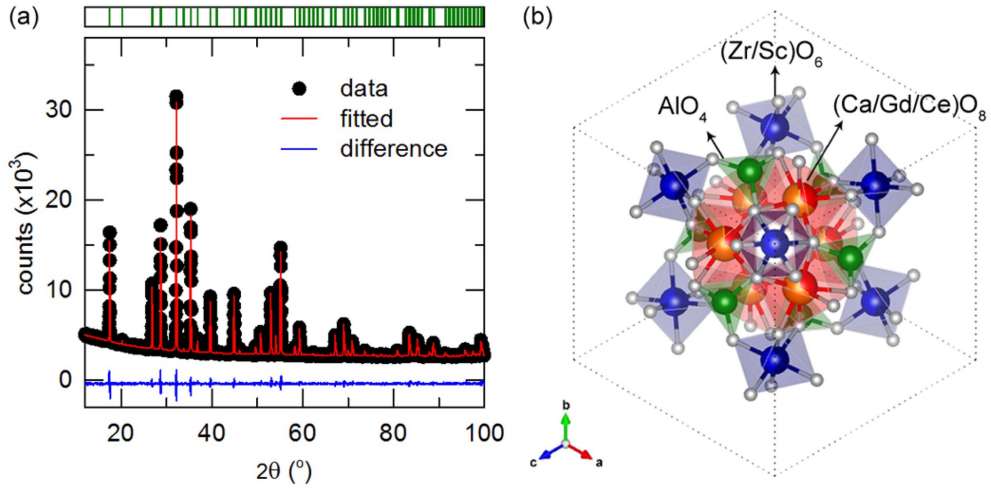

Fig. 1. (a) Rietveld refinement of the powder X-ray diffraction profile of $CaGd_2ZrSc(AlO_4)_3$:0.04Ce^{3+} phosphor. Data (points), fit (lines), difference profile, and expected reflection positions are displayed. (b) Schematic of the crystal structure of the $CaGd_2ZrSc(AlO_4)_3$:0.04Ce^{3+} phosphor viewed in the [111] direction.

Table 1. Rietveld Refinement and Crystal Data of $CaGd_2ZrSc(AlO_4)_3$:0.04Ce^{3+} Obtained Using X-ray Diffraction

Formula	$CaGd_{1.96}Ce_{0.04}ZrSc(AlO_4)_3$
radiation type	CuKα
T/K	295
2θ range (degree)	10 - 100
symmetry	cubic
space group	*Iα*-3*d* (#230)
a, *b*, *c*/Å	12.46417(5)
volume/Å^3	1936.378(23)
Z	8
R_p	1.74%
R_{wp}	2.60%
χ^2	2.261

When Ce^{3+} ions are incorporated into the crystal structure of CGZSA, Ce^{3+} ions may substitute at all cationic sites, i.e., Ca^{2+}, Gd^{3+}, Zr^{4+}, Sc^{3+}, and Al^{3+}. However, considering their corresponding ionic radius and allowed oxygen-coordination number (*n*), i.e., Ca^{2+} (1.12 Å, *n* = 8), Gd^{3+} (1.053 Å, *n* = 8), Zr^{4+} (0.72 Å, *n* = 6), Sc^{3+} (0.745 Å, *n* = 6), and Al^{4+} (0.39 Å, *n* = 4), it is difficult for Ce^{3+} ions (1.01 Å, *n* = 6 and 1.143 Å, *n* = 8) to substitute for Zr^{4+}, Sc^{3+}, and Al^{3+} ions.[16] The BVS of the structure refinement of CGZSA:0.04Ce^{3+} suggested that the BVS for Ca^{2+} is close to the expected value, and the determined Gd^{3+}/Ce^{3+} site provides a slightly underbonded location for Gd^{3+} with BVS = 2.747, whereas Ce^{3+} is lightly overbonded with BVS = 3.153. This explains the preference of Ca, Gd, and Ce for the 24*c* site; placing all the Gd and Ce at the 24*c* site with Ca provides sensible atomic displacement parameters for this site.

Figure 2 shows the powder XRD patterns of the samples with $0.01 \le x \le 0.07$ in CGZSA:*x*Ce^{3+} and the simulated XRD pattern of CGZSA from the Rietveld refinement data for comparison. The XRD patterns of the samples are consistent with their corresponding simulated XRD patterns. Although the ionic radius of Gd^{3+} (1.053 Å, *n* = 8) is smaller than that of Ce^{3+} (1.143 Å, *n* = 8), the peak of XRD did not shift as the amount of Gd^{3+} replaced by Ce^{3+} increased, as shown in Fig. 2(b). This result shows that the amount of Ce^{3+} ions was only slightly substituted for and no significant change was observed.

Figure 3(a) presents the excitation and emission spectra of

Table 3. Selected Bond Lengths (Å) and Bond Valence Sums for $CaGd_2ZrSc(AlO_4)_3$:0.04$Ce^{3+\alpha}$

dodecahedron	
Gd/Ca/Ce-O	2.4080(34)
Gd/Ca/Ce-O[3)]	2.4080(34)
Gd/Ca/Ce-O[9)]	2.4080(34)
Gd/Ca/Ce-O[11)]	2.4080(34)
Gd/Ca/Ce-O[7)]	2.5217(32)
Gd/Ca/Ce-O[1)]	2.5217(32)
Gd/Ca/Ce-O[10)]	2.5217(32)
Gd/Ca/Ce-O[13)]	2.5217(32)
BVS of dodecahedron	Ca = 2.017, Gd = 2.747, Ce = 3.153
octahedron	
Zr/Sc-O[1)]	2.090(5)
Zr/Sc-O[2)]	2.090(5)
Zr/Sc-O[3)]	2.090(5)
Zr/Sc-O[4)]	2.090(5)
Zr/Sc-O[5)]	2.090(5)
Zr/Sc-O[6)]	2.090(5)
BVS of octahedron	Zr = 3.970, Sc = 3.128
tetrahedron	
Al-O	1.759(4)
Al-O[8)]	1.759(4)
Al-O[9)]	1.759(4)
Al-O[12)]	1.759(4)
BVS of tetrahedron	Al = 2.956

[a]Symmetry transformations used to generate equivalent atoms: [1)]+*y*+3/4, +*x*+1/4, –*z*+1/4, [2)]–*x*+3/4, –*z*+3/4, –*y*+3/4, [3)]+*z*+1/4, –*y*+1/4, +*x*+3/4, [4)]+*x*+3/4, +*z*+3/4, +*y*+3/4, [5)]–*z*+1/4, +*y*+1/4, –*x*+3/4, [6)]–*y*+3/4, –*x*+1/4, +*z*+1/4, [7)]–*z*+1/2, –*x*, +*y*+1/2, [8)]–*z*+1/4, –*y*+3/4, +*x*+3/4, [9)]–*x*+1/2, +*y*, –*z*, [10)]+*z*, –*x*, –*y*+1/2, [11)]–*z*+1/4, –*y*+1/4, –*x*+1/4, [12)]+*z*+1/4, –*y*+3/4, –*x*+1/4, [13)]–*y*+3/4, +*x*+1/4, +*z*+3/4

Table 2. Refined Structural Parameters for $CaGd_2ZrSc(AlO_4)_3$:0.04Ce^{3+} Derived from Rietveld Refinement Using X-ray Powder Diffraction Patterns at Room Temperature[a]

atom	Wyck.	*x*	*y*	*z*	*g*[b]	100 × U_{iso}[c]/Å^2
Ca	24*c*	¼	⅝	0	0.330	0.603
Gd	24*c*	¼	⅝	0	0.656	0.603
Ce	24*c*	¼	⅝	0	0.014	0.603
Zr	16*a*	¼	¾	¼	0.500	0.525
Sc	16*a*	¼	¾	¼	0.500	0.525
Al	24*d*	¼	⅜	0	1	0.396
O	96*h*	0.3447(4)	0.4652(23)	0.0530(28)	1	0.426

[a]The numbers in parentheses are the estimated standard deviations of the last significant figure. [b]Constraint on occupancy: *g*(Ca) + *g*(Gd) + *g*(Ce) = 1 and *g*(Zr) + *g*(Sc) = 1. [c]Constraint on isotropic thermal factor: U_{iso}(Ca) = U_{iso}(Gd) = U_{iso}(Ce) and U_{iso}(Zr) = U_{iso}(Sc).

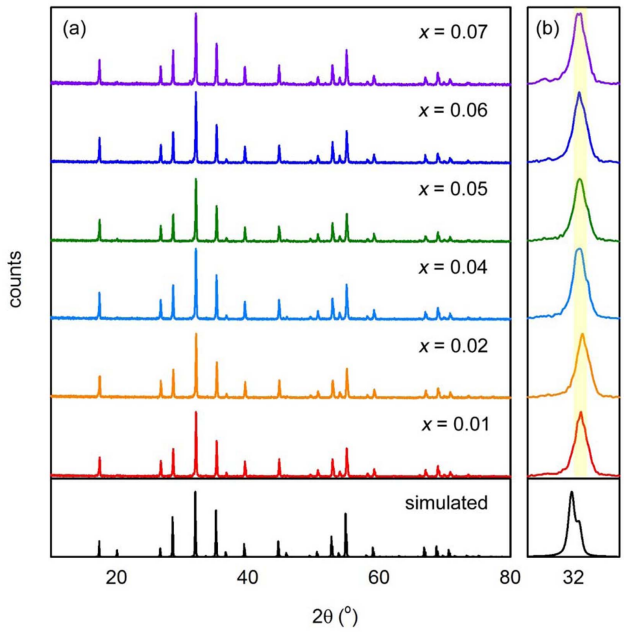

Fig. 2. (a) X-ray diffraction pattern of $CaGd_{2-x}ZrSc(AlO_4)_3:xCe^{3+}$ (x = 0.01 - 0.07) phosphors. As a reference, the simulated XRD for $CaGd_2ZrSc(AlO_4)_3:0.04Ce^{3+}$ is shown. (b) Magnified XRD pattern in the region between 31.5° and 32.5° for the $CaGd_{2-x}ZrSc(AlO_4)_3:xCe^{3+}$ phosphor as a function of Ce^{3+} concentration.

the CGZSA:xCe^{3+} (x = 0.01 - 0.07) phosphors. The excitation band was observed at 450 nm. The exhibited shapes of the excitation and emission bands decrease in intensity and there is a red-shift of the maximum wavelength with an increase in the Ce^{3+} concentration due to reabsorption of emitted photons by the activator. Fig. 3(b) shows the excitation and emission spectra of the optimized CGZSA:0.04Ce^{3+} under excitation at 440 nm at room temperature. The excitation spectrum was separated into two excitation bands of Ce^{3+}–a $5d_1$ band between 370 and 500 nm, and a $5d_2$ band level between 300 nm and 360 nm–which are assigned the two lowest $5d$ levels of Ce^{3+} and which are attributed to the crystal field splitting. The intensity of the $5d_2$ band was less than two times that of the $5d_1$ band owing to symmetry selection rules.[17] Similarly, the PL spectrum involves a broad asymmetric emission band related to the spin-allowed d-f transition of Ce^{3+} with its maximum at the wavelength of 541 nm under excitation at 440 nm.

The dependence of the emission intensity on the Ce^{3+} substitution is shown in Fig. 3(c). We observed that the optimum substitution of Ce^{3+} in CGZSA:xCe^{3+} was x = 0.04. When x exceeds 0.04, a decrease in the relative emission intensity was observed owing to concentration quenching. Generally, concentration quenching is mainly caused by non-radiative energy transfer processes from one Ce^{3+} ion to

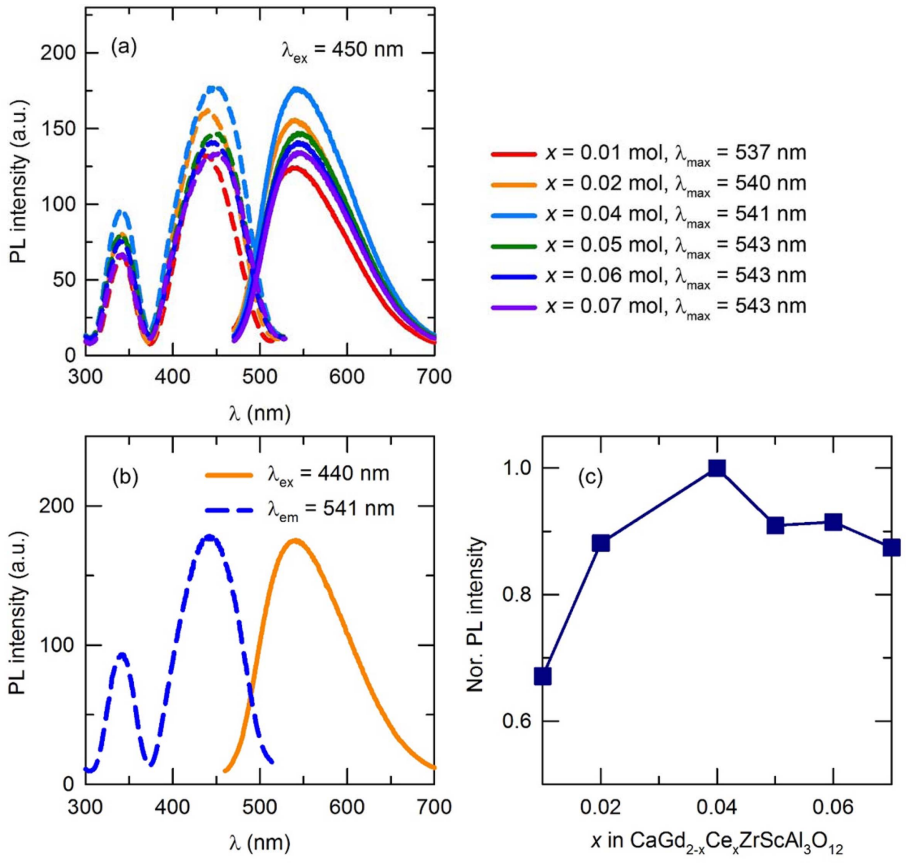

Fig. 3. (a) Excitation and emission spectra of $CaGd_{2-x}ZrSc(AlO_4)_3:xCe^{3+}$ (x = 0.01 - 0.07) phosphors. (b) Excitation and emission spectra of the $CaGd_2ZrSc(AlO_4)_3:0.04Ce^{3+}$ phosphor. (c) Relative emission intensity as a function of Ce^{3+} substitution, x.

another Ce^{3+} ion. Non-radiative energy transfer usually occurs as a result of exchange interaction, radiation reabsorption, or electric multipolar interaction.[18] According to the Dexter theory, the mechanism of radiation re-absorption occurs only when there is a broad overlap of excitation and emission spectra. To further investigate the concentration quenching mechanism of the CGZSA:0.04Ce^{3+} phosphor, the critical transfer distance (R_c) was roughly estimated. In this case, to further determine the energy transfer mechanism, R_c between Ce^{3+} activators can be estimated using the following formula: [19]

$$R_C \approx 2\left(\frac{3V}{4\pi X_C N}\right)^{1/3} \quad (1)$$

where V corresponds to the volume of the unit cell, N is the number of total Ce^{3+} sites per unit cell, and X_c is the critical concentration of dopant ions. For the CGZSA:0.04Ce^{3+} phosphor, on the basis of the structural parameters, we used the values V = 1936.378 Å^3, N = 24, and X_c = 0.04 (see Table 1). R_c for the energy transfer in the CGZSA:Ce^{3+} phosphor was calculated and found to be approximately 15 Å.

Based on the spectral data of the CGZSA:0.04Ce^{3+} phosphor, we also used the Dexter formula, expressed as follows, to calculate R_c. The formula represents a confined transfer of electric dipole-dipole interaction, and is suitable because we herein assumed dipole-allowed transitions in the case of Ce^{3+}. The probability of transfer of dipole-dipole interaction has been given by Blasse:[19,20]

$$R_C^6 = 0.63 \times 10^{28} \frac{4.8\times10^{-16}P}{E^4} \int f_s(E)F_A(E)dE \quad (2)$$

where P is the oscillator or strength of the Ce^{3+} ion, E is the energy of the maximum spectral overlap, and the integral represents a spectral overlap, which is the product of the normalized spectral shapes of the emission and excitation. The values of E and $\int f_s(E)F_A(E)dE$ were derived from the spectral data in Fig. 2(a) as 2.53 eV and 4.8 × 10^{-2} eV^{-1}, respectively. The value of P corresponding to the broad 4*f*–5*d* absorption band was obtained as 10^{-2} from Blasse. From equation (2), the value of R_c for the energy transfer in the CGZSA:0.04Ce^{3+} phosphor was calculated and found to be 18 Å, which is close to the value of 15 Å obtained using the concentration quenching data. According to Blasse, the value of R_c for the general exchange interaction is ~ 5 Å.[18] Therefore, the exchange interaction can be neglected in the energy transfer within the CGZSA:0.04Ce^{3+} phosphor.

Via structural analysis, we confirmed that the Ce^{3+} ions occupied only the Gd site and, via PL measurement at low temperature (–196°C), we confirmed that they generated two peaks in the PL spectra due to the variation of the emission spectra, as shown in Fig. 4. The emission band of the phosphor was deconvoluted into two Gaussians profiles with peaks centered at 528 nm (18938 cm^{-1}) and 581 nm (17222 cm^{-1}). The difference between the two values is 1716 cm^{-1}. Essentially, the Ce^{3+} ion, with $4f^1$ ground state configuration of $^2F_{5/2}$ and $^2F_{7/2}$, allows two levels whose maxima

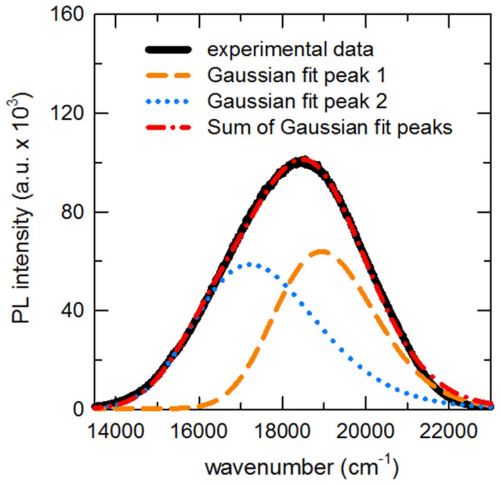

Fig. 4. Deconvoluted PL emission spectra obtained using two Gaussian equations for the $CaGd_2ZrSc(AlO_4)_3$:0.04Ce^{3+} phosphor at –196°C (λ_{ex} = 375 nm).

were isolated in a range of 1600 to 2000 cm^{-1} as a result of spin–orbit coupling.[18] Therefore, using the two Gaussians for the deconvolution of the emission peak resulted in a reasonable value of fitting, as shown in Fig. 4.

The lifetime of the CGZSA:0.04Ce^{3+} phosphor was calculated by analyzing the decay curves presented in Fig. 5. The normalized decay profile of the CGZSA:0.04Ce^{3+} phosphor was measured under excitation at 450 nm and by monitoring the emission peak at 541 nm. It was observed that the decay curve fitted well with second-order exponential decay, which can be obtained using the equation:

$$I(t) = I_0 + A_1 \exp^{(-t/\tau_1)} + A_2 \exp^{(-t/\tau_2)} \quad (3)$$

where $I(t)$ is the luminescence intensity, t is the time, A_1 and A_2 are constants, and τ_1 and τ_2 are the decay times of the

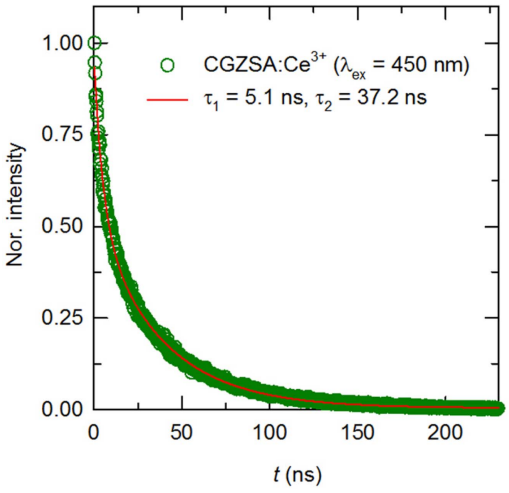

Fig. 5. Decay curve of Ce^{3+} emission in the $CaGd_2ZrSc(AlO_4)_3$:0.04Ce^{3+} phosphor under excitation at 450 nm, monitored at 541 nm.

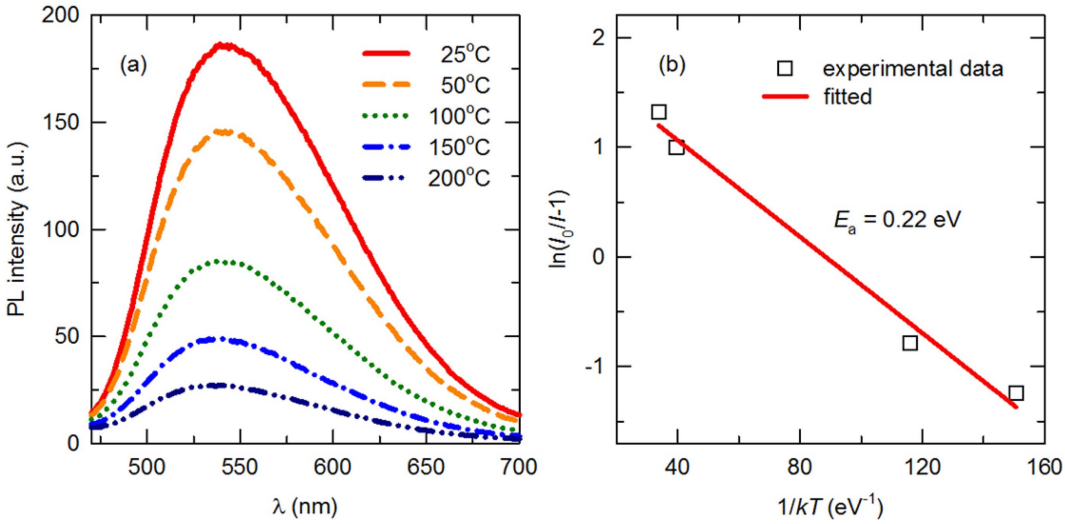

Fig. 6. (a) PL spectra of the $CaGd_2ZrSc(AlO_4)_3:0.04Ce^{3+}$ phosphor under various temperatures (25 - 200°C) and (b) plots of fitted activation energy for thermal quenching.

exponential components. The decay profile of the CGZSA:0.04Ce^{3+} phosphor shows rapid components (τ_1 = 5.1 ns) and slow time (τ_2 = 37.2 ns). Further, $5d \rightarrow 4f$ fluorescence transitions of the Ce^{3+} ions are the allowed electric dipole-dipole and their fluorescence lifetimes are in the time range of 10 - 100 ns owing to local changes of the crystal field.[21] The presence of the fast component indicates the existence of a non-radiative process from the excited Ce^{3+} to the quenching centers, such as structural defects and local distortions in crystals.[22] The slow component is in accordance with the intrinsic lifetime of Ce^{3+} in the CGZSA: 0.04Ce^{3+} phosphor.

The TQ property is an important parameter for the practical applications of phosphors. Fig. 6(a) shows the thermal quenching characteristics of the CGZSA:0.04Ce^{3+} phosphor in the temperature range of 25 to 200°C. It can be observed that the emission intensity of CGZSA:0.04Ce^{3+} decreases rapidly with the increase in temperature, and only approximately 46% of the emission intensity recorded at room temperature remains at 100°C. Furthermore, it can be observed that, with the increase in temperature, the emission intensity decreases gradually and the emission band changes from two apparent asymmetric broad peaks to one definite broadband. In order to explain the large TQ behavior of the CGZSA:0.04Ce^{3+} phosphor, two possible models in Ce^{3+}-doped phosphors are considered, as follows. One model, the well-known non-radiative relaxation model, is explained by using a configurational coordinate diagram (CCD), wherein the excited luminescence center is thermally activated through phonon interaction and released through the crossing point between the excited and ground states. This non-radiative transition probability *via* thermal activation is strongly dependent on the temperature, and results in a decrease in the emission intensity.[23] Owing to the increasing phonon interaction and the non-radiative transition with the increase in temperature, the spectral overlap between the excitation band and the first emission band increases. The other model is the thermal ionization model.[24] Thermal ionization refers to a thermally activated electron transfer process to the conduction band.

Further, in order to investigate the TQ characteristics, the activator energy (E_a) was calculated using the Arrhenius equation, shown below:[25]

$$I(T) = \frac{I_0}{1 + A \exp\left(\frac{-E}{kT}\right)} \quad (4)$$

where I_0 is the initial intensity, $I(T)$ is the intensity at a given temperature T, A is a constant, E is the activation energy for TQ, and k is the Boltzmann constant. Through the best fit using the Arrhenius equation, the activation energy (E) was obtained as 0.22 eV for the CGZSA:0.04Ce^{3+} phosphor, as shown in Fig. 6(b). The activation energy of the YAG:Ce^{3+} phosphor was determined to be approximately 0.77 eV.[24] This indicates that the CGZSA:0.04Ce^{3+} phosphor has a cross-point in the CCD lower than that of the YAG:Ce^{3+} phosphor. The thermal emission stability decreases owing to the reduction of the energy displacement between the host conduction band and the Ce^{3+} 5*d* band levels. Moreover, the host, which includes Gd ions, has a large non-radiative transition in the garnet structure owing to the weak crystal structure of the host and, hence, the energy relaxation from the excited state to the ground state has a large loss due to lattice vibration.[26] Further, the value of QY of the CGZSA:0.04Ce^{3+} phosphor, measured at room temperature, was 20%. The value of QY is also related to ΔE_a; hence, it would be lower in the phosphor with stronger luminescence TQ.

4. Conclusions

Yellow CGZSA:*x*Ce^{3+} phosphors were successfully prepared using a solid-state reaction. The phase purity was

characterized using XRD analysis. Under excitation at 440 nm, the CGZSA:0.04Ce^{3+} phosphor showed a bright yellow emission peak at approximately 541 nm. The PL properties, QY, and thermal stability of the CGZSA:0.04Ce^{3+} phosphor were investigated in detail to evaluate their use in LEDs. Therefore, it can be concluded that the yellow CGZSA:*x*Ce^{3+} phosphor is a promising material that can be employed in pc-WLEDs for solid-state lightning.

Acknowledgments

This work was financially supported by the Basic Science Research Program through the National Research Foundation of Korea (NRF), funded by the Ministry of Science, ICT & Future Planning (NRF-2017R1A2B3011967).

REFERENCES

1. C. Feldmann, T. Jüstel, C. R. Ronda, and P. J. Schmidt, "Inorganic Luminescent Materials: 100 Years of Research and Application," *Adv. Funct. Mater.*, **13** [7] 511-16 (2003).
2. K. S. Y. Shimizu, Y. Noguchi, and T. Moriguchi, "Light Emitting Device Having a Nitride Compound Semiconductor and a Phosphor Containing a Garnet Fluorescent Material"; US Patent 5,998,925, (July 29, 1999).
3. G. Blasse and A. Bril, "A New Phosphor for Flying-Spot Cathode-ray Tubes for Color Television: Yellow-emitting $Y_3Al_5O_{12}$-Ce^{3+}," *Appl. Phys. Lett.*, **11** [2] 53-55 (1967).
4. The Nobel Prize in Physics 2014. http://www.nobelprize.org/nobel_prizes/physics/laureates/2014/. Accessed on 20/09/2017.
5. J. C. Krupa and M. Queffelec, "UV and VUV Optical Excitations in Wide Band Gap Materials Doped with Rare Earth Ions: 4*f*–5*d* Transitions," *J. Alloy. Compd.*, **250** [1-2] 287-92 (1997).
6. P. Dorenbos, "5*d*-level Energies of Ce^{3+} and the Crystalline Environment. IV. Aluminates and "Simple" Oxides," *J. Lumin.*, **99** [3] 283-99 (2002).
7. G. A. Novar and G. V. Grnns, "The Crystal Chemistry of the Silicate Garnets," *Am. Mineral.*, **56** 791-825 (1971).
8. F. Euler and J. A. Bruce, "Oxygen Coordinates of Compounds with Garnet Structure," *Acta Crystallogr.*, **19** [6] 971-78 (1965).
9. Y. Shimomura, T. Honma, M. Shigeiwa, T. Akai, K. Okamoto, and N. Kijima, "Photoluminescence and Crystal Structure of Green-Emitting $Ca_3Sc_2Si_3O_{12}$:Ce^{3+} Phosphor for White Light Emitting Diodes," *J. Electrochem. Soc.*, **154** [1] J35-38 (2007).
10. G. Blasse and A. Bril, "Investigation of Some Ce^{3+}-Activated Phosphors," *J. Chem. Phys.*, **47** [12] 5139-45 (1967).
11. A. A. Setlur, W. J. Heward, Y. Gao, A. M. Srivastava, R. G. Chandran, and M. V. Shankar, "Crystal Chemistry and Luminescence of Ce^{3+}-Doped $Lu_2CaMg_2(Si,Ge)_3O_{12}$ and Its Use in LED Based Lighting," *Chem. Mater.*, **18** [14] 3314-22 (2006).
12. X. Gong, J. Huang, Y. Chen, Y. Lin, Z. Luo, and Y. Huang, "Novel Garnet-Structure $Ca_2GdZr_2(AlO_4)_3$:Ce^{3+} Phosphor and Its Structural Tuning of Optical Properties," *Inorg. Chem.*, **53** [13] 6607-14 (2014).
13. A. C. Larson and R. B. V. Dreele, "General Structure Analysis System (GSAS)," Los Alamos National Laboratory Report LAUR 86-748, September 2004.
14. N. E. Brese and M. O'Keeffe, "Bond-Valence Parameters for Solids," *Acta Crystallogr. B*, **47** [2] 192-97 (1991).
15. A. Yoshiasa, A. Nakatsuka, and M. Ohkawa, "EXAFS Study on the Short-Range Correlation of Vibrational Motion in the $Y_3Fe_{5-x}Ga_xO_{12}$ Garnet Solid Solution," *Min. Jour.*, **19** [1] 21-32 (1997).
16. R. Shannon, "Revised Effective Ionic Radii and Systematic Studies of Interatomic Distances in Halides and Chalcogenides," *Acta Crystallogr. A*, **32** [5] 751-67 (1976).
17. D. J. Robbins, "The Effects of Crystal Field and Temperature on the Photoluminescence Excitation Efficiency of Ce^{3+} in YAG," *J. Electrochem. Soc.*, **126** [9] 1550-55 (1979).
18. G. Blasse and B. C. Grabmaier, Luminescent Materials; Vol. 1, pp. 70-90, Springer, Berlin Heidelberg, 1994.
19. G. Blasse, "Energy Transfer In Oxidic Phosphors," *Philips Res. Rep.*, **24** 131-44 (1969).
20. D. L. Dexter, "A Theory of Sensitized Luminescence in Solids," *J. Chem. Phys.*, **21** [5] 836-50 (1953).
21. J. A. Mares and M. Nikl, "Energy Transfer, Fluorescence and Scinitillation Processes in Cerium-doped $RE^{3+}AlO_3$ Fast Scintillators," *Acta Phys. Pol. A*, **90** [1] 45-54 (1996).
22. D. J. Robbins, B. Cockayne, J. L. Glasper, and B. Lent, "The Temperature Dependence of Rare-Earth Activated Garnet Phosphors: I. Intensity and Lifetime Measurements on Undoped and Ce-Doped $Y_3Al_5O_{12}$," *J. Electrochem. Soc.*, **126** [7] 1213-20 (1979).
23. Y. H. Kim, P. Arunkumar, B. Y. Kim, S. Unithrattil, E. Kim, S.-H. Moon, J. Y. Hyun, K. H. Kim, D. Lee, J.-S. Lee, and W. B. Im, "A Zero-Thermal-Quenching Phosphor," *Nat. Mater.*, **16** [5] 543-50 (2017).
24. J. Ueda, P. Dorenbos, A. J. J. Bos, A. Meijerink, and S. Tanabe, "Insight into the Thermal Quenching Mechanism for $Y_3Al_5O_{12}$:Ce^{3+} through Thermoluminescence Excitation Spectroscopy," *J. Phys. Chem. C*, **119** [44] 25003-8 (2015).
25. Y. Chen, B. Liu, C. Shi, G. Ren, and G. Zimmerer, "The Temperature Effect of Lu_2SiO_5:Ce^{3+} Luminescence," *Nucl. Instrum. Meth. A*, **537** [1] 31-5 (2005).
26. C.-C. Chiang, M.-S. Tsai, and M.-H. Hon, "Luminescent Properties of Cerium-Activated Garnet Series Phosphor: Structure and Temperature Effects," *J. Electrochem. Soc.*, **155** [6] B517-20 (2008).